Femtosecond Laser Ablation of Thin Films on Substrate

N. A. Inogamov[1], V. A. Khokhlov[1], V. V. Zhakhovsky[2], Yu. V. Petrov[1,3], K. V. Khishchenko[2], and S. I. Anisimov[1]

[1]L.D. Landau Institute for Theoretical Physics of Russian Academy of Sciences, Russian Federation
[2]Joint Institute for High Temperatures of Russian Academy of Sciences, Russian Federation
[3]Moscow Institute of Physics and Technology, Russian Federation

Abstract— Our targets are thin (60–100 nm thick) plane metal films (here gold is considered) on a dielectric substrate (fused silica below). We consider laser action onto such targets. A femtosecond laser pulse with durations 30–300 fs is used. Thermal and mechanical behavior of those targets qualitatively differs from behavior of bulk targets and from freestanding films. A weakly conductive substrate works as a heat insulating wall if we compare the bulk target and the film/silica target, thus slowing down cooling of metal due to the heat conduction loses into bulk. While hydromechanical interaction of the film with the silica changes the situation in comparison with the freestanding case when both sides of a film are vacuum boundaries. From the one hand, the silica counteracts against an expansion of metal into the glass. From the other hand, a cohesion force between the metal and silica resists to separation of film from substrate. Situations with the bulk targets and freestanding films were studied before. In the paper for the first time we present descriptions of possible regimes of film/silica dynamics. They depend on absorbed fluence, two-temperature physics, and a value of a cohesion force. Electrons are much hotter than ions at a two-temperature stage. Two-temperature effects are dynamically significant because in case of gold with its delayed electron-ion relaxation the electron pressure contributes into momentum of a film while an electron conductivity (enhanced at a two-temperature stage) together with a rate of electron energy transfer into ion subsystem define energy redistribution across a thickness of a film.

1. INTRODUCTION

In many applications an ultrashort laser pulse irradiates thin films deposited onto a dielectric substrate. E.g., microbumping and lifting phenomena caused by blistering and ejection of the irradiated film are important for laser bio-printing and LIFT (Laser Induced Forward or Backward Transfer) technologies [1–3], for formation of arrays of nanoholes [4], and for nanophotonics/nanoplasmonics applications (e.g., creation of nanoantennas [5]). The case with a film on substrate is interesting and, as it was said, important. Indeed, a system with a thin film between a substrate from the one side and vacuum from the other side is very different from a case of bulk targets [6–10] and from a case of a freestanding (both boundaries are free) thin film [9, 11–14] studied previously. There are papers devoted to an analysis of phenomena connected with a contact boundary between two media both having finite inertia (not the vacuum — condensed phase contact). The items considered in those papers are: dynamics of an aluminum-glass boundary irradiated through glass [15, 16]; impact of metal onto a dielectric producing a shock in substrate, rarefaction in a metal, and a sharp deceleration of an expansion of hot metal [17, 18]; and motion of a metal-liquid surface heated by a femtosecond laser pulse through liquid [19, 20].

But the ablation regimes when the *both* contact boundaries of a thin film are strongly dynamically interacting (like in the freestanding thin film) and one of the boundaries is a contact with medium with a finite acoustic impedance were not described. In the paper below the systems named a "film on substrate" are considered in details. Interplay of rarefaction waves in a film and dynamic interaction between the film and the substrate define motion after irradiation. It is shown below that there are three regimes of behavior depending mainly on absorbed energy F_{abs}, a cohesion stress p_{coh}, and thickness of film d_f, where the stress p_{coh} defines a cohesion between two media at a contact. Under weak illumination $F < F_{abl}$ the *whole* (i.e., uncut) film remains at substrate (the regime 1). In this case the film loses its momentum and a small part of accumulated thermal energy oscillating on a substrate and radiating a chain of decaying acoustic waves into a thick substrate. The larger part of the thermal energy is lost as a result of slow cooling due to weak heat conductivity of a substrate and due to radiative loses from a free surface. Those oscillations have been observed experimentally [21].

We consider the case of a large ratio of acoustic impedances of contacting media (gold on fused silica [3]) and rather weak cohesion. Then there is an interval of fluences $F_{abl} < F < F_{sp}$ where

a film separates (delaminates) as a whole from a substrate (the regime 2). The third regime exists if a fluence is above the spallation threshold F_{sp}. Then a film breaks in its internal part. Both thresholds F_{abl} and F_{sp} are connected with mechanical breaking under action of tensile stress and therefore both maybe called spallation (e.g., contact spallation and internal spallation). The both thresholds are higher than a melting threshold (if p_{coh} is not too small). Let us clarify that sometimes peoples connect spallation only with breaking of solids while breaking of liquid is called cavitation. The schemes of the three regimes are presented in Fig. 1.

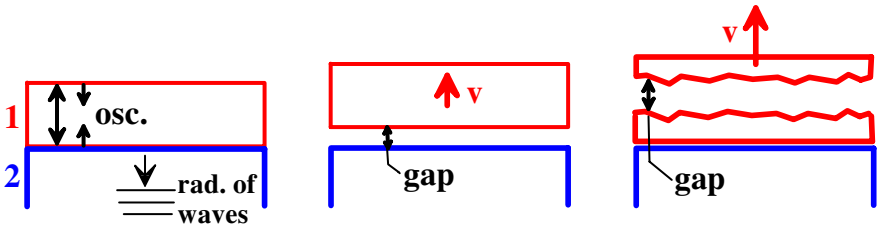

Figure 1: From left to right: regimes 1, 2, and 3. The film is "1", the substrate is "2". Regime 1: the film exhibits gradually decaying oscillations on the substrate; a chain of acoustic waves, caused by those oscillations, propagates into the bulk of the substrate. Regime 2: the film delaminates from the substrate, the growing gap appears between them, velocity v of the film increases with fluence [3]. Regime 3: the breaking takes place inside the film. A solitary acoustic wave is emitted into substrate in the regimes 2 and 3.

2. OSCILLATIONS OF FILM

Modern model of two-temperature physics [22–24] is used in our simulations presented below. It includes one-temperature equations of thermodynamical states for gold and silica taken from [25]. Two-temperature system of hydrodynamic equations used here is described, e.g., in [22]. It combines thermal and dynamic equations and thus differs from the classical two-temperature thermal system (developed first in [26]) involving only heat equations for an electron and ion subsystems. We show that for the $d_f = 60$–$100\,\mathrm{nm}$ thick gold films the electron-ion temperature relaxation time scale $t_{eq} \sim 7\,\mathrm{ps}$ and the acoustic time scale $t_s = d_f/c_s \sim 20$–$30\,\mathrm{ps}$ are comparable. Here d_f and c_s are film thickness and speed of sound. Electrons become much hotter than ions $(T_e - T_i)/T_i \gg 1$ during a laser pulse. Temperature difference $(T_e - T_i)/T_i$ gradually decreases due to an electron-ion thermal coupling. The two-temperature stage finishes when the difference becomes small $|T_e - T_i|/T_i < 1$. Duration of a two-temperature stage defines a scale t_{eq}. An electron-ion coupling parameter [23], conductivity [23, 24], and a two-temperature equation of state [22] are dynamically important for the flow evolution.

Figure 2 presents results of simulation for $F_{abs} = 30\,\mathrm{mJ/cm^2}$, $d_f = 100\,\mathrm{nm}$, duration of a pulse is $\tau_L = 100\,\mathrm{fs}$. A laser pulse has illuminated the vacuum boundary. This value of F_{abs} for 100 nm film is 5% below the lower boundary of the melting interval on the axis F_{abs}. For both cases considered in Figs. 2 and 3 a film remains solid. The interval of melting appears as a result of (i) approximately homogeneous ion temperature distribution established after a two-temperature stage across a film, (ii) a finite difference in the enthalpy between the solid and liquid states of metal. The cohesion stress p_{coh} taken for those simulations overcomes maximum tensile stress at a contact. For simulation presented in Figs. 2 and 3(a) this means that $p_{coh} > 1.24$ GPa, and $p_{coh} > 0.68$ GPa for the case shown in Figs. 3(b) and 3(c). A tensile stress inside a film does not achieve a strength limit for gold for those temperatures and those deformation rates therefore a film remains intact.

Figure 2 demonstrates an evolution caused by the counter propagation of the vacuum rarefaction wave (RW) and the contact RW. In Fig. 2(a) the vacuum RW moves from left to right and the contact RW moves from right to left. Fig. 2(b) shows the hydrodynamic situation after reflections of RWs from the boundary with vacuum (contact RW) and from the contact (vacuum RW). In Fig. 2(b) the RWs change directions: the vacuum RW moves from right to left, while the contact RW moves from left to right. In Fig. 2(a) pressure inside a film decreases from plus to minus, while in Fig. 2(b) pressure gradually increases.

It is curious that a similar growth of pressure (around a breaking layer) follows the breaking, when also the compression waves (spallation pulses) begin to propagate from the breaking point.

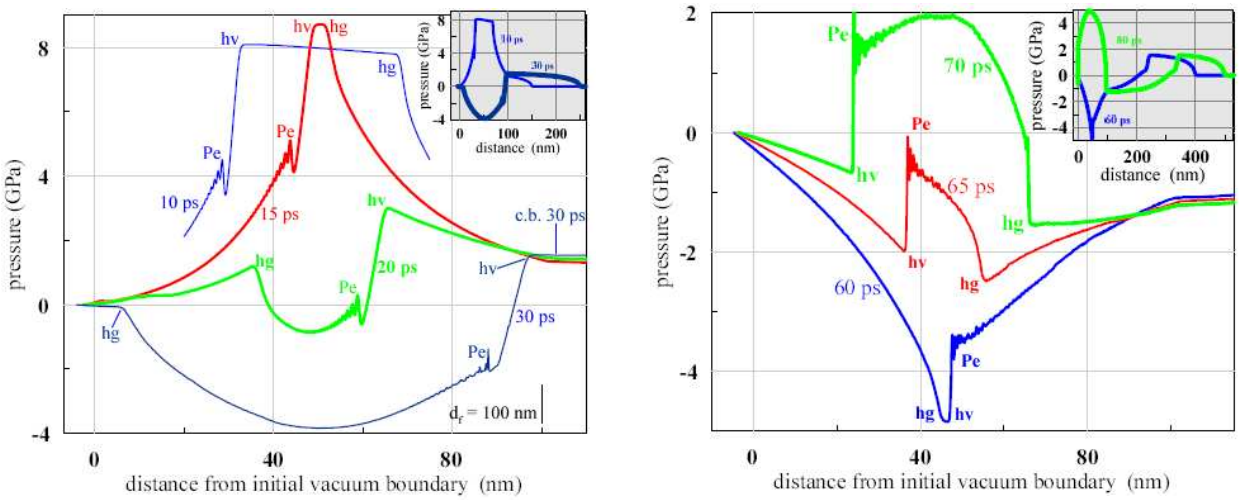

Figure 2: (a) Convergence of the rarefaction waves (RWs) and their passing through each other inside the film. Initial positions of vacuum and glass boundaries correspond to the points $x = 0$ and $x = 100\,\text{nm}$. The head characteristics of the RW starting from the vacuum boundary is "hv" (head vacuum), "Pe" is the trace of a sharp peak in electron pressure traveling along characteristics after creation of the peak at the boundary with vacuum. In time this peak of electron pressure is lasting few hundreds femtoseconds covering a duration of a laser pulse. The head characteristics of a rarefaction wave propagating from the contact with glass is "hg" (head glass). Every RW drops pressure down. In this figure pressure mainly decreases with time. At the instant $t = 15\,\text{ps}$ the "hv" and "hg" heads are near their first intersection. After the intersection the both amplitudes add together and therefore a drop of pressure to the negative values begins. At the instant 30 ps the heads "hv" and "hg" are near the boundaries of a film. Soon a reflections of the RWs from the boundaries will begin. Position of the contact at 30 ps is marked as "c.b. 30 ps". (b) Propagation of the reflected RWs: 60 ps is an instant just before the second intersection of the heads "hv" and "hg". After reflection from the boundaries the RWs change their polarity. Therefore after the second intersection, the summation of the RWs increases pressure from negative to positive values (in this figure pressure increases with time). In this connection, please pay attention to the reverse relation between the pressure profiles for instants 15 and 60 ps. Comparing the traveling durations, we see that stretching decreases speed of sound. Therefore the duration between the first and second intersections is not $\approx 30\,\text{ps}$ but $\approx 45\,\text{ps}$. We also see, how a compression wave becomes steeper during propagation as result of nonlinearity. The insets show propagation of the wave irradiated from the film into the glass.

But in the case of breaking the growth of pressure is limited by the zero value, while in the case shown in Fig. 2(b) the pressure continues to grow to the high positive values.The breaking case takes place at the stage of stretching (Fig. 2(a)) when two rarefactions add each other, while Fig. 2(b) corresponds to the stage of compression when two compression waves add each other. The stage of stretching is the first quarter of the whole period of oscillation, the stage of compression is the next quarter.

3. BREAKING OR CONTACT, OR FILM BUT USUALLY NOT BOTH

Breaking is connected to a finite strength of material to resist to its stretching. Condensed matter breaks if a tensile stress overcomes the finite value of its strength p_{str}. This finite value defines a threshold because an amplitude of a tensile stress increases with fluence F_{abs}. Situation with the thermomechanical breaking in case of a bulk target is well understood [6–10]. Breaking of a thin film quickly (supersonically) homogeneously heated is also studied well [9, 11–14]. Situation is more complicated if a depth d_T heated by ultrashort pulse is thinner than a film $d_T < d_f$ [9].

Let's consider the case named a "film on substrate" when a film covers a substrate. We suppose that the strength of a contact p_{coh} cannot be larger than a strength of a substrate. Then there are two possibilities: at the lowest threshold F_{thr} a system "film on substrate" breaks or at the contact, or inside the film.

The internal tensile stress is always (here we restrict ourself to the case of the large ratio of the impedances) higher than the contact tensile stress, see Fig. 3(a). This means that if the contact

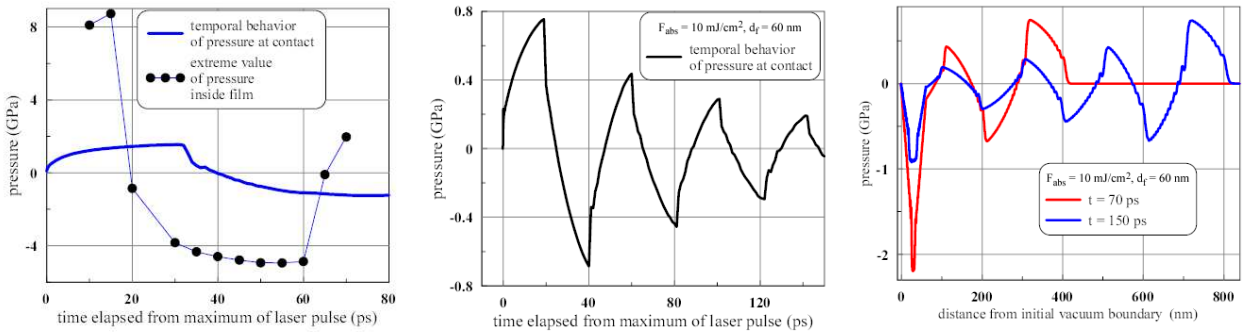

Figure 3: (a) Comparison of temporal dependencies of pressures at a contact and inside a film is shown. To plot the extreme value of an internal pressure, we take the maximum value of pressure inside a film when the whole pressure profile inside a film is positive, see Fig. 2. And we take the minimum value of pressure when the negative values appear at the pressure profile, see Fig. 2. We conclude that, firstly, absolute values of the internal pressures are always higher than pressures at a contact. This is consequence of a large impedance difference between gold and silica. Therefore stress field in a film is higher than stresses outside, see also Fig. 3(c). Secondly, the strongest internal tensile stresses are always achieved *before* the instants when the strongest contact tensile stresses are achieved. All this have important consequences for the cases above the thresholds F_{abl} or F_{sp}, see next Chapters. In acoustic approximation a wave propagating into glass is $p(x - c_s t)$. Therefore the temporal behavior at a contact $x = x_{\text{contct}}$ in Fig. 3(a) is similar to the spatial profile of pressure in glass in the inset in Fig. 2(b) for the instant 80 ps. (b) $F_{abs} = 10\,\text{mJ/cm}^2$, $d_f = 60\,\text{nm}$. Gradual decay of oscillations of pressure at a contact. Oscillations decay as result of irradiation of acoustic energy into substrate, see next figure. (c) Propagation into glass of a chain of acoustic signals irradiated by an oscillating film. Amplitude of oscillation inside a film is always higher than the irradiated amplitude because at the contact the main part of acoustic energy is reflected back into a film.

p_{coh} and internal p_{str} strengths are comparable (or $p_{coh} > p_{str}$) then contact never will be ruptured.

Gold is weakly connected to a fused silica, thus at the lowest threshold F_{thr} the system breaks at the contact. Above two thresholds have been introduced. One (F_{abl}) corresponds to a contact, and may be called also F_{contct}, while the other (F_{sp}) corresponds to a film and may be called F_{film}. We have $F_{abl} \equiv F_{\text{contct}} < F_{sp} \equiv F_{\text{film}}$ in the case with a weak cohesion between a film and a substrate.

Why the second (higher) threshold $F_{sp} \equiv F_{\text{film}}$ appears in the case with a weak cohesion? Indeed, the delamination of the film varies the hydrodynamic flow in comparison with the unbroken case. But we should remember that the maximum stretching inside a film is created *prior* to the maximum stretching of a contact, see Fig. 3(a). Therefore above the second threshold $F_{sp} \equiv F_{\text{film}}$ the internal breaking takes place in advance to the instant when the maximum stretching at a contact will be achieved.

The event of the internal breaking qualitatively changes the hydrodynamic situation. It cuts short the oscillation behavior inside the first quarter of the oscillation, then irradiation of a chain of acoustic waves shown in Fig. 3(c) stops. But the main consequence of the internal rupture is that it reverse the direction of momentum acting onto a contact. Without the rupture the vacuum RW pulls a contact producing a tensile stress at a contact. While after the internal breaking a film is divided to two part. The external (i.e., adjoined to vacuum) part gains momentum directed to vacuum, while the internal part gains momentum directed to silica. It may be shown that in this case the tensile stress at a contact cannot be created. The internal part of a gold film gradually loses its momentum as a result of deceleration by a low density silica substrate. The deceleration lasts few acoustic time scales $t_s = d_f/c_s$. It is longer if the ratio of impedances is larger.

Thus in the case of the large ratio of impedances and the weak cohesion p_{coh} there are three regimes changing each other (see Fig. 1) as fluence grows.

ACKNOWLEDGMENT

The work was supported by the Russian Foundation for Basic Research, grant No. 13-08-01095.

REFERENCES

1. Ivanov, D. S., et al., "Short laser pulse nanostructuring of metals: Direct comparison of molecular dynamics modeling and experiment," *Appl. Phys. A*, Vol. 111, 675–687, 2013.

2. Emelyanov, V. I., D. A. Zayarniy, et al., "Nanoscale hydrodynamic instability in a molten thin gold film induced by femtosecond laser ablation," *JETP Lett.*, Vol. 99, No. 9, 518–522, 2014.
3. Inogamov, N. A., V. V. Zhakhovsky, et al., "Jet formation in spallation of metal film from substrate under action of femtosecond laser pulse," *JETP*, Vol. 120, No. 1, 15–48, 2015.
4. Nakata, Y., N. Miyanaga, and T. Okada, "Topdown femtosecond laser-interference technique for the generation of new nanostructures," *J. Phys.: Conf. Ser.*, Vol. 59, 245–248, 2007.
5. Gubko, M. A., et al., "Enhancement of ultrafast electron photoemission from metallic nanoantennas excited by a femtosecond laser pulse," *Laser Phys. Lett.*, Vol. 11, 065301, 2014.
6. Inogamov, N. A., Yu. V. Petrov, S. I. Anisimov, A. M. Oparin, et al., "Expansion of matter heated by an ultrashort laser pulse," *JETP Lett.*, Vol. 69, No. 4, 310–316, 1999.
7. Volkov, A. N. and L. V. Zhigilei, "Hydrodynamic multi-phase model for simulation of laser-induced non-equilibrium phase transformations," *J. Phys.: Conf. Ser.*, Vol. 59, 640–645, 2007.
8. Gill-Comeau, M. and L. J. Lewis, "Ultrashort-pulse laser ablation of nanocrystalline aluminum," *Phys. Rev. B*, Vol. 84, 224110, 2011.
9. Demaske, B. J., V. V. Zhakhovsky, N. A. Inogamov, and I. I. Oleynik, "Ablation and spallation of gold films irradiated by ultrashort laser pulses," *Phys. Rev. B*, Vol. 82, 064113, 2010.
10. Starikov, S. V. and V. V. Pisarev, "Atomistic simul. of laser-pulse surface modif.: Predictions of models with various length and time scales," *J. Appl. Phys.*, Vol. 117, 135901, 2015.
11. Zhakhovskii, V. V., K. Nishihara, et al., "Molecular-dynamics simulation of rarefaction waves in media that can undergo phase transitions," *JETP Lett.*, Vol. 71, No. 4, 167–172, 2000.
12. Anisimov, S., V. Zhakhovskii, N. Inogamov, and K. Nishihara, "Destruction of a solid film under the action of ultrashort laser pulse," *JETP Lett.*, Vol. 77, No. 11, 606–610, 2003.
13. Anisimov, S. I., V. V. Zhakhovskii, et al., "Simulation of the expansion of a crystal heated by an ultrashort laser pulse," *Appl. Surf. Sci.*, Vol. 253, No. 15, 6390–6393, 2007.
14. Upadhyay, A. K., et al., "Ablation by ultrashort laser pulses: Atomistic and thermodynamic analysis of the processes at the ablation threshold," *Phys. Rev. B*, Vol. 78, 045437, 2008.
15. Agranat, M. B., et al., "Strength properties of an aluminum melt at extremely high tension rates under the action of femtosecond laser pulses," *JETP Lett.*, Vol. 91, No. 9, 471–477, 2010.
16. Inogamov, N., V. Zhakhovskii, S. Ashitkov, et al., "Laser acoustic probing of two-temperature zone created by femtosecond pulse," *Contrib. Plasma Phys.*, Vol. 51, No. 4, 367–374, 2011.
17. Evans, R., A. D. Badger, et al., "Time- and space-resolved optical probing of femtosecond-laser-driven shock waves in aluminum," *Phys. Rev. Lett.*, Vol. 77, No. 16, 3359–3362, 1996.
18. Inogamov, N. A., V. V. Zhakhovsky, V. A. Khokhlov, and V. V. Shepelev, "Superelasticity and the propagation of shock waves in crystals," *JETP Lett.*, Vol. 93, No. 4, 226–232, 2011.
19. Povarnitsyn, M. E., et al., "Mechanisms of nanoparticle formation by ultra-short laser ablation of metals in liquid environment," *Phys. Chem. Chem. Phys.*, Vol. 15, 3108–3114, 2013.
20. Karim, E. T., M. Shugaev, Ch. Wu, Zh. Lin, R. F. Hainsey, and L. V. Zhigilei, "Atomistic simulation study of short pulse laser interaction with a metal target under conditions of spatial confinement by a transparent overlayer," *J. Appl. Phys.*, Vol. 115, 183501, 2014.
21. Wang, J. and C. Guo, "Non-equilibrium electronic Gruneisen parameter," *Appl. Phys. A*, Vol. 111, 273–277, 2013.
22. Petrov, Yu. V., K. P. Migdal, N. A. Inogamov, and V. V. Zhakhovsky, "Two-temperature equation of state for aluminum and gold with electrons excited by an ultrashort laser pulse," *Appl. Phys. B*, DOI: 10.1007/s00340-015-6048-6, 2015.
23. Petrov, Yu. V., N. A. Inogamov, and K. P. Migdal, "Thermal conductivity and the electron-ion heat transfer coefficient in condensed media with a strongly excited electron subsystem," *JETP Lett.*, Vol. 97, No. 1, 20–27, 2013.
24. Petrov, Yu. V., N. A. Inogamov, and K. P. Migdal, "Two-temperature heat conductivity of gold," *PIERS Proceedings*, sent to Proceedings, 2015.
25. http://www.ihed.ras.ru/rusbank/.
26. Anisimov, S. I., B. L. Kapeliovich, and T. L. Perel'man, "Electron emission from metal surfaces exposed to ultrashort laser pulses," *Sov. Phys.-JETP*, Vol. 39, No. 2, 375–377, 1974.